SUPPLEMENTARY INFORMATION:

Single-cell topological RNA-Seq analysis reveals insights into cellular differentiation and development

Abbas H. Rizvi[1†], Pablo G. Camara[2,3†], Elena K. Kandror[1], Thomas J. Roberts[1,3], Ira Schieren[4], Tom Maniatis[1*], and Raul Rabadan[2,3*]

[1] Department of Biochemistry and Molecular Biophysics,

[2] Department of Systems Biology,

[3] Department of Biomedical Informatics,

[4] Howard Hughes Medical Institute,

Columbia University Medical Center,

New York, NY 10032.

*Correspondence to: rr2579@cumc.columbia.edu, tm2472@columbia.edu

†These authors contributed equally to this work

Supplementary Tables

	Diffusion pseudotime	Wishbone	SLICER	Destiny	Monocle	SCUBA	scTDA
Unbiased	No	No	Yes	Yes	No	No	Yes
Statistics	Yes*	Yes*	Yes*	No	Yes*	Yes*	Yes
Exploits longitudinal information	No	No	No	No	No	Yes	Yes
Reference	6	7	8	9	10	11	-

* Only for branching events

Supplementary Table 1. Comparison of various features among existing algorithms for single-cell RNA-seq data analysis.

Supplementary Table 2 (Provided as a separate spreadsheet). Characterization of the expression profile in the topological representation of the two motor neuron differentiation experiments for all RefSeq genes. For each gene and experiment, the number of nodes with non-zero expression, the mean, minimum and maximum expression values, the value of the gene connectivity, the statistical significance before (*p*-value) and after (*q*-value) adjusting for the false discovery rate (Benjamini-Hochberg), the centroid and dispersion (expressed in days), and the gene group assignment are presented. Several gene ontology annotations are also shown.

Supplementary Table 3 (Provided as a separate spreadsheet). Gene ontology enrichment analysis for each gene group in the two motor neuron differentiation experiments. Statistical significant ($q < 0.05$, Bonferroni) biological process gene ontologies are presented for each gene group in the topological representation.

Supplementary Table 4 (Provided as a separate spreadsheet). Characterization of the expression profile in the topological representation of the two motor neuron differentiation experiments for significant lncRNAs. For each antisense or intergenic NONCODEv4 lncRNA with significant ($q < 0.05$) gene connectivity in both experiments gene and experiment, the number of nodes with non-zero expression, the mean, minimum and maximum expression values, the value of the gene connectivity, the statistical significance before (p-value) and after (q-value) adjusting for the false discovery rate (Benjamini-Hochberg), the centroid and dispersion (expressed in days), the gene group assignment, and the number of reads in bulk stranded RNA-seq data from days 2 to 6 of the differentiation are presented. Alternate RefSeq name is shown, when available. For antisense lncRNAs, the name of the coding genes in the opposite strand is presented. Only lncRNAs supported by at least 50 reads in one day of the bulk stranded RNA-seq data are considered.

Supplementary Table 5 (Provided as a separate spreadsheet). Characterization of the expression profile in the topological representation of 80 embryonic (E18.5) mouse lung

epithelial cells. For each gene, the number of nodes with non-zero expression, the mean, minimum and maximum expression values, the value of the gene connectivity, and the statistical significance before (*p*-value) and after (*q*-value) adjusting for the false discovery rate (Benjamini-Hochberg), are presented.

Supplementary Table 6 (Provided as a separate spreadsheet). Characterization of the expression profile in the topological representation of 1,529 individual cells from 88 human preimplantation embryos. For each gene, the number of nodes with non-zero expression, the mean, minimum and maximum expression values, the value of the gene connectivity, the statistical significance before (*p*-value) and after (*q*-value) adjusting for the false discovery rate (Benjamini-Hochberg), the centroid and dispersion (expressed in days), and the gene group assignment are presented.

Supplementary Table 7 (Provided as a separate spreadsheet). Characterization of the expression profile in the topological representation of 272 newborn neurons from the mouse neocortex. For each gene, the number of nodes with non-zero expression, the mean, minimum and maximum expression values, the value of the gene connectivity, the statistical significance before (*p*-value) and after (*q*-value) adjusting for the false discovery rate (Benjamini-Hochberg), the centroid and dispersion (expressed in days) are presented.

Supplementary Table 8 (Provided as a separate spreadsheet). Barcoded reverse transcription primers utilized in motor neuron differentiation experiment 2.

Supplementary Note 1

A mathematical primer.

In this note some of the fundamental mathematical objects used to study single cell expression data are further explained. scTDA builds upon recent developments in topological data analysis, or TDA. The over arching aim of TDA is to infer global properties of spaces from samples of points. Most of the constructions in TDA are based on generating sets of simplicial complexes (generalizations of networks) and exploit the global structure of these complexes. In particular, we are interested in a space that is a simplified, lower dimensional version of the original space. In 1904[1] Poincare called this concept the skeleton of the space, or in more modern terms, a Reeb graph or space[2,3]. A Reeb graph is a graph (a one dimensional object) that summarizes some, but not necessarily all, topological features of a space, like number of connected components or loops. Mapper is the algorithm developed by Singh, Memoli, and Carlsson[4] that constructs simplicial complexes from finite metric spaces (points with distances) as approximations to Reeb spaces.

We are interested in studying dynamic biological processes (like development or evolution) from samples of points, reconstructing and inferring properties of the underlying or some derived spaces (as Reeb spaces), showing how these properties relate to time, and studying functions on these spaces by performing statistical analysis. Although TDA is able to represent, summarize and quantify properties of spaces from finite sampling, TDA is not adapted to study dynamical processes or to perform statistical analysis on functions on associated objects (e.g. simplicial complexes). The primary intellectual contributions of this paper are the following: to extend the construction of Reeb spaces in finite metric spaces with temporal sampling, to study statistics on

functions defined on the data, and to apply these methods in the context of single cell transcriptomic data.

Starting from single cell transcriptomic data, the final reconstructed object is an annotated simplicial complex, with a single vertex labeling the initial state and statistics associated with functions on the data. The marked single point in the construction allows the association of a real-valued function to the rest of the complex representing the imputed pseudotime. The statistics on functions on the simplicial complex measure how expression profiles are localized.

Simplicial complexes and topological data analysis.

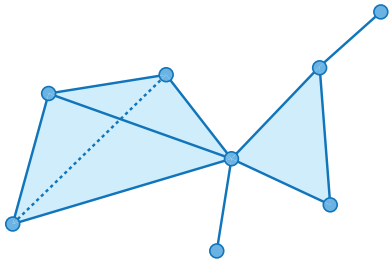

The final object we calculate is an annotated simplicial complex together with statistics associated to functions defined on the complex. The basic "atomic" objects that compose a simplicial complex are simplices. An n-dimensional simplex spanned by points $[v_0, v_1, \ldots, v_k]$ is the convex hull of k+1 affine-independent points in $\mathbb{R}^n$. A zero-dimensional simplex is just a point, a one-dimensional simplex a line segment, a two-dimensional simplex a triangle, a three dimensional a tetrahedron, etc. Each n-simplex is a collection of n+1 points, n(n+1)/2 lines joining the points, etc. Simplicial complexes are collections of simplices of different dimensions (see figure). Indeed, a simplicial complex can be defined as a set of simplices with the property that a non-empty intersection between two simplices in the set is a face in each of the two simplices forming the intersection.

Most of data, including most of biological data, and certainly the data from single cell expression, can be presented as a set of points (e.g. cells) with some notion of similarity or distance (e.g. similarity between expression profiles), i.e. these data constitute a finite metric space (X, ∂). We can associate different simplicial complexes with the data. For instance, consider a scale ε at which we are going to study our data and define the Vietoris-Rips complex VRε(X, ∂) as

1. vertices are the points of X, and

2. a simplex $[v_0, v_1, \ldots, v_k]$ is in the complex when $\partial(v_i, v_j) < \varepsilon$ for all $0 \leq i, j \leq k$.

Topological Data Analysis (or TDA) refers to a set of techniques to characterize the topological properties of data. Typically it involves constructing an auxiliary set of objects, e.g. simplicial complexes.

Morse functions, Reeb graphs and Reeb spaces.

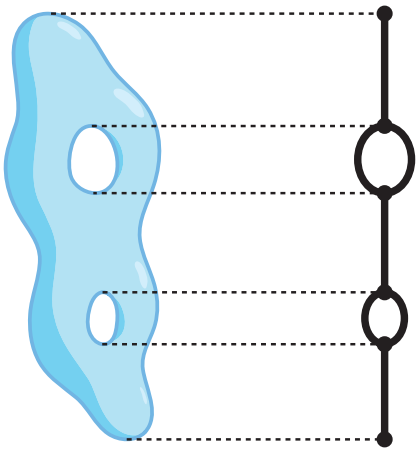

Imagine that we have a topological space *M*, as in the left side of the figure, and a continuous function f : *M* -> $\mathbb{R}$. Let us define an equivalence relation on M between two points p ~ q in *M* if f(p)=f(q) and p and q in the same connected component in $f^{-1}(p)$. The Reeb graph associated to the space M and the function f is Reeb(*M*,f) = *M*/~, the quotient of M by the above equivalence relation (see figure). The first mention of this construction was in the 5th Supplement of the funding paper of topology (Analysis Situs) from 1904. Poincare referred to the Reeb graph of a manifold as the skeleton.

One can generalize the notion of Reeb graph to Reeb spaces by considering functions f: M -> $\mathbb{R}^n$. Using the above equivalence relation one can define Reeb(M,f) = M/~. In the applications to single cell data we will be only using n=1 and n=2.

Mapper as an approximation to Reeb spaces.

The data that we will considering in single cell analysis can be understood as points in a high dimensional space with some notion of similarity between them (X, ∂). We can approximate the "skeleton" or Reeb space of these data by considering an auxiliary function f: X -> $\mathbb{R}^n$. The Mapper algorithm generates a simplicial complex Mapper(X, ∂,C) from (X, ∂, f) and C={U_i}, a cover on the image of f in $\mathbb{R}^n$.

Several types of covers are possible, depending on specific applications. The Mapper algorithm proceeds as follows:

1.- Cluster the elements of $f^{-1}(U_i)$, the inverse image of each element in the cover. Let us denote each of the clusters by C_μ.

2.- Vertices of Mapper(X, ∂,C) are the clusters C_μ from 1. and a simplex [C_0, C_1,…, C_k] is in the simplicial complex Mapper(X, ∂,C) when the (k+1)-fold intersection of elements in {C_0, C_1,…, C_k} is not empty.

The results of Mapper can be considered as an approximation of Reeb spaces. Indeed, the work of Elizabeth Munch and Bei Wang have shown the convergence of Mapper and Reeb graphs[5].

Weinberger theorems.

One natural question is how many points we should sample to get a "good" approximation to the topology of the original space. Without any assumption on connectivity, Weinberger[6] estimated the number of topological types (potential solution to the topology inference problem, which could be in this context homeomorphisms, diffeomorphisms or homotopy type) from finite sampling in a manifold of dimension n embedded in $\mathbb{R}^N$. These estimates depend on a scale number, called the condition number (the minimum size at which a tubular neighborhood self-intersects) and the diameter of the manifold (D) measure in units of the scale number (so is dimensionless). For dimension, n=0 (clusters) or n=1 (graphs) the number grows as D^N, while for n=2 the number of types grows like $\exp(D^{N/2})$, and for N>2 $\exp(D^N)$. Notice that the problem has a polynomial on size only for inference of low dimensional objects (clusters and graphs), but become exponential on the diameter for higher dimensions. Even to express the right answer, one needs many bits (on the order of log of the number of possibilities), so one needs at least O(N log(D)) points in dimension 0 and 1, $O(D^{N/2})$ for dimension 2 and $O(D^N)$ for higher dimensions. That implies that in our single cell experiments, where N, the embedding dimension (number of genes used in the reconstruction) is of the same order as the number of cells, we can only aim to capture 0 or 1 dimensional features. Notice that the exponential of number of genes will be always be bigger than the atoms in the universe, then bigger than the number of cells in the universe, so we will never reach the complexity needed for characterizing the topology type in dimension bigger than 1. These obstacles become even more daunting when interested in estimating additional structure (local coordinates, metric structure, etc) as in some manifold learning procedures.

These results that one is more likely to be successful to identify low dimensional features of spaces (likes clusters of graphs) that to capture higher dimensional ones. We have two advantages in this direction. First is a technical one. Inference of Reeb graphs or clustering should be easier with finite number of points. Second is a biological presumption. When looking at single cell data we expect data to come in clusters (different cell types) and trajectories (like lineage differentiation, or evolution). These theoretical and practical implications suggest that a potential approach to study single cell data should be through the study of low dimensional objects, as the approximation of Reeb graphs that Mapper generates. However, the Mapper reconstructed complexes lack annotation regarding time and statistics associated to functions on it, that are fundamental for an application to single cell applications.

Studying temporal single cell data, scTDA.

scTDA builds upon Mapper to generate an simplicial complex that captures some of the low dimensional features from the space (like clusters and trajectories) from single cell data. One of the main ideas described in this manuscript is how to use the temporal information to find a single vertex in the inferred complex that represents the closest point to the most “ancestral” state. This ancestral node could be a stem cell state, progenitor, embryonic state, cancer initiating cell, etc. The idea, explained throughout the manuscript, is based on the association between the graph distance from a node and the measured time. The ancestral state is defined as the node that maximizes this correlation. The details are explained in Results and Methods sections of the manuscript.

The second fundamental point in our applications, and in many others as well, is the identification of some features in the space. That requires to study functions from data to real numbers, g: X -> $\mathbb{R}$ and statistics associated to them. In our case, these functions could the expression of genes or phenotypic observations in single cells, and we are interested in identifying transcriptional programs associated to states, such as genes expressed on the cell membrane, that could work as markers. A simple idea is to construct functions on the simplicial complex by averaging functions on X over the points representing each simplex (in each cluster). That defines a kind of pushforward of the function on the original data to a function on the simplicial complex g~: Mapper(X, ∂, f, C) -> $\mathbb{R}$. Statistics are defined by permuting the values of the function on the original data, and comparing the pushforward of the permuted values with the original ones. The details for the single cell analysis are described in the manuscript.

Using scTDA, we refine TDA simplicial representations by providing a marked state, a derived pseudotime, a set of pushforward functions g~ on the complex and statistics associated to them.

Homology in simplicial complexes and persistent homology.

Now that we have an annotated simplicial complex representing the data and functions on it, we can further use topological tools to characterize the presence of different topological tools on them. In particular, in our applications, we have used simplicial homology and persistent homology. The basic idea of simplicial homology is to associate groups with objects of different dimension. The zero dimensional homology captures the number of connected components in a simplicial complex in the following fashion: we say that two zero simplices a and b are in the same equivalence class

a~b if they are the boundary of a chain of one dimensional objects (i.e. if there is a path connecting a and b). The same procedure can be defined to objects of higher dimension: closed loops are related if they form the boundary of two dimensional objects, etc. The rank of the homology groups, or Betti numbers, captures the number of independent components of different dimensions that are in the space. The first Betti number counts the number of loops in a space.

When working with finite metric spaces (X, ∂) one can define a set of related simplicial complexes in the following fashion. At each scale ε one can define a simplicial complex (for instance, the Vietoris-Rips complex VRε(X, ∂)). At a bigger scale ε'> ε one can define a different complex that will include the scale at complex $VR\epsilon(X,\partial) \hookrightarrow VR\epsilon'(X,\partial)$. This allows to track the different chains of objects at different scales and to identify the relevant scales at which different homology classes are present. A summary of the different scales at which homology classes are present is capture by the notion of a barcode: a multiset of non-empty intervals of the form either $[a_i, b_i) \subset \mathbb{R}$ or $[a_i, \infty)$, representing the scales when the homology class h_i is present. Notice that the zero dimensional homology shows how different clusters are joined as the scale ε increases, and it is formally equivalent to single linkage clustering. The presence of a barcode [a, b) in one dimensional persistent homology, on the other hand, shows the scales $\epsilon \in [a, b)$ at which there is a loop in the data.

As we show in the manuscript, both simplicial and persistent homology are useful tools to data mine the results from the analysis. We encourage the interested reader to read about the topic in introductory textbooks for simplicial homology[7] and textbooks and reviews on persistent homology[8, 9].

References

1. Poincare, H. Cinquième complément à l'analysis situs. *Palermo Rend.* **18**, 45-110 (1904).
2. Adelson-Velskii, G. & Kronrod, A. in Dokl. Akad. Nauk SSSR, Vol. 49 239-241 (1945).
3. Reeb, G. Sur les points singuliers d'une forme de Pfaff completement intégrable ou d'une fonction numérique. *CR Acad. Sci. Paris* **222**, 2 (1946).
4. Singh, G., Mémoli, F. & Carlsson, G.E. in SPBG 91-100 (Citeseer, 2007).
5. Munch, E. & Wang, B. Convergence between categorical representations of Reeb space and mapper. *arXiv preprint arXiv:1512.04108* (2015).
6. Weinberger, S. The complexity of some topological inference problems. *Foundations of Computational Mathematics* **14**, 1277-1285 (2014).
7. Hatcher, A. Algebraic topology. *Cambridge UP, Cambridge* **606** (2002).
8. Carlsson, G. Topology and data. *Bulletin of the American Mathematical Society* **46**, 255-308 (2009).
9. Edelsbrunner, H. & Harer, J. Computational topology: an introduction. (American Mathematical Soc., 2010).

Supplementary Note 2

Single cell library generation

In one biological replicate, we sorted a small sample size from a differentiation, sequencing 80 cells per differentiation time-point utilizing standard CEL-Seq primers with anchor bases at the 3' end of reverse transcription primers, pooling 40 cells at a time prior to *in vitro* transcription (IVT). To assess library saturation and capture efficiency, two single cell libraries from each differentiation time point (consisting of 40 cells each) from the experiment 1 were paired end sequenced (2x125 bps) on an Illumina HiSeq 2500, operating in high output mode, sequencing

with Illumina v4 chemistry. To increase capture efficiency, enhanced *in vitro* transcription based amplification, and leveraging the library saturation curves from experiment 1, we utilized 96 barcoded CEL-Seq RT primers (**Supplementary Table 4**), forgoing the usage of anchor bases at the 3' terminus. We then conducted a differentiation on a second biological replicate, sampling 384 cells per time-point (inclusive of 96 FACS purified mid-level GFP expressing, and 288 high GFP expressing cells), collected into 96 well plates and implemented CEL-Seq, now pooling 96 cells per IVT reaction. Following IVT, aRNA was fragmented using magnesium (NEBNext Magnesium RNA Fragmentation Module) for 90 seconds and column purified (Zymo Research RNA Clean & Concentrator-5). Purified aRNA was then subjected to treatment with Antarctic Phosphatase and T4 polynucleotide kinase. Ligation of Illumina RA3 adapters was conducted using truncated T4 RNA Ligase 2 for 1 hour at 28 C. Following adapter ligation, adapter ligated aRNA was reverse transcribed using Illumina RTP at 50 C for 1 hour and placed on ice. To avoid amplification based batch effects, the resultant cDNA was PCR amplified with Illumina RPIX primers to no more than 15 cycles. The sequencing libraries were then twice purified using AmpureXP beads, held at a ratio of 1:0.65, yielding size selected libraries with an insert size of ~250 bps. The single cell libraries were then multiplexed to a total representation of 384 cells per lane at equimolar concentrations and mixed with 50% exome libraries generated using an Illumina TruSeq Exome Kit.